Acute in vivo exposure to interferon-γ enables resident brain dendritic cells to become effective antigen presenting cells

Andres Gottfried-Blackmore[a], Ulrike W. Kaunzner[a], Juliana Idoyaga[b], Jennifer C. Felger[a], Bruce S. McEwen[a], and Karen Bulloch[b,1]

Laboratories of [a]Neuroendocrinology and [b]Cellular Physiology and Immunology, The Rockefeller University, New York, NY 10065

Contributed by Bruce S. McEwen, October 7, 2009 (sent for review July 30, 2009)

Dendritic cells (DC) are the professional antigen presenting cells (APC) that bridge the innate and adaptive immune system. Previously, in a CD11c/EYFP transgenic mouse developed to study DC functions, we anatomically mapped and phenotypically characterized a discrete population of EYFP$^+$ cells within the microglia that we termed brain dendritic cells (bDC). In this study, we advanced our knowledge of the function of these cells in the CD11c/EYFP transgenic mouse and its chimeras, using acute stimuli of stereotaxically inoculated IFNγ or IL-4 into the CNS. The administration of IFNγ increased the number of EYFP$^+$bDC but did not recruit peripheral DC into the CNS. IFNγ, but not IL-4, upregulated the expression levels of major histocompatibility class II (MHC-II). In addition, IFNγ-activated EYFP$^+$bDC induced antigen-specific naïve CD4 T cells to proliferate and secrete Th1/Th17 cytokines. Activated bDC were also able to stimulate naïve CD8 T cells. Collectively, these data reveal the Th1 cytokine IFNγ, but not the Th2 cytokine IL4, induces bDC to up-regulate MHC-II and become competent APC.

Dendritic cells (DC), the professional antigen presenting cells (APC) of the immune system, can process antigens and traffic to lymphoid organs to activate antigen-specific naïve T cells, thereby bridging innate and adaptive immunity (1). Differentiated DC typically express CD11c and have moderate to high surface levels of major histocompatibility class II (MHC-II), which can be further elevated upon activation (2). In unchallenged animals, CD11c$^+$MHC-II$^+$ cells are undetectable by immunocytochemistry in the brain parenchyma, but have been noted in the perivascular spaces, meninges, and choroid plexus (3).

Recently, using a CD11c/EYFP transgenic mouse developed to study DC function (4), we identified, in the steady state, a unique population of EYFP$^+$, CD11b$^+$, MHC-II^{neg} ramified cells in various regions of the developing and adult brain parenchyma that we termed brain dendritic cells (bDC) (5). Although localized to discrete anatomical brain regions, these bDC share a remarkable morphologic and phenotypic similarity with microglia (MG) (5), raising the possibility that these cells might be derived from this highly heterogeneous population (6). In fact, the phenotype of resting MG, characterized by low levels of CD45, MHC, and co-stimulatory molecules (7), has led some authors to suggest that among the microglia there may be CD11b$^+$ DC precursors (8, 9). These studies, limited to in vitro cell cultures from developing brains, have shown that activated microglia can re-stimulate previously activated T cells (10–12), a function common to many activated macrophages. However, the ability of adult brain MG to stimulate naive CD4 T cells, a function of DC, has yet to be established.

Interferons (IFN) type I and II are critical mediators of innate and adaptive immune responses and are involved in the development/differentiation of mouse DC, particularly the conventional CD11b$^+$ subsets (13). IFN type II, also known as IFN-gamma (IFNγ), originates primarily from functionally mature CD4 T-helper–1 (Th1) T cells and is part of the cascade of cytokines and events culminating in a robust adaptive immune response. IFNγ is particularly effective as an inducer of MHC proteins, which are essential components of adaptive immunity.

Within the central nervous system (CNS), IFNγ can induce MHC class I (MHC-I) and MHC-II expression in some parenchymal cells (14–17), most notably in MG (10, 11, 18). IFNγ receptors have also been detected on resting adult MG (10). Moreover, IFNγ, as well as interleukin-4 (IL-4), has been reported to induce CD11c and MHC-II expression in primary MG cultures (19), suggesting that IFNγ is capable of stimulating some MG to adopt a DC phenotype.

Although it is well established that the expression of MHC can be upregulated both experimentally and pathologically in the CNS, the capacity of different cell types to express MHC proteins and become effective APCs is still controversial (20). Chronic inflammatory conditions such as neurodegenerative disorders (21, 22), experimental autoimmune encephalitis (EAE) (23), infection (8), and even chronic cytokine infusions (24), are reported to produce a significant increase of bone marrow–derived (peripheral) DC in the brain. Typically, these DC express high levels of CD45, an accepted marker for brain-infiltrating leukocytes. However, the contribution of a brain-resident APC has not been identified in these disease states because of insufficient markers for their presence. In the present study, we used intracerebral injection of the Th1 cytokine (IFNγ) in the CD11c/EYFP transgenic mouse, and herein provide in vivo evidence that a brain-resident EYFP$^+$ APC can be induced from a subpopulation of MG. Furthermore, the EYFP$^+$bDC were significantly more potent activators of naïve CD4 T cells than the EYFP negative MG (EYFP^{neg}MG).

Results

IFNγ Induces a Large Increase of CD11c/EYFP$^+$ Cells in the Brain. To analyze the effects of a single cytokine on brain parenchymal MG and bDC without the confounding effects of systemic inflammation or activation of the peripheral immune system, recombinant IFNγ was stereotaxically injected (10 ng in 0.5 μl) directly into the CA1 area of the hippocampus, a region where EYFP$^+$bDC are rare at this age. Twenty-four hours postinoculation of IFNγ, a robust increase of EYFP$^+$bDC was induced in the ipsilateral brain hemisphere extending far beyond the injection site. This increase peaked at 2 days and declined by day 4 postinjection (Fig. 1*A*). In the saline control (Sal), EYFP$^+$cells were only evident juxtaposed to the puncture wound induced by the needle tract (Fig. 1*A*). Morphologically, all EYFP$^+$bDC resembled activated microglia (25) (Fig. 1*A Inset*), and expressed the bDC markers CD11b and Iba1 (5).

Flow-cytometric analysis from whole-brain preparations, exclud-

Author contributions: A.G.-B., J.I., and K.B. designed research; A.G.-B., U.W.K., and J.C.F. performed research; A.G.-B. and J.I. analyzed data; and A.G.-B., B.S.M., and K.B. wrote the paper.

The authors declare no conflict of interest.

[1]To whom correspondence should be addressed. E-mail: bulloch@rockefeller.edu.

This article contains supporting information online at www.pnas.org/cgi/content/full/0911509106/DCSupplemental.

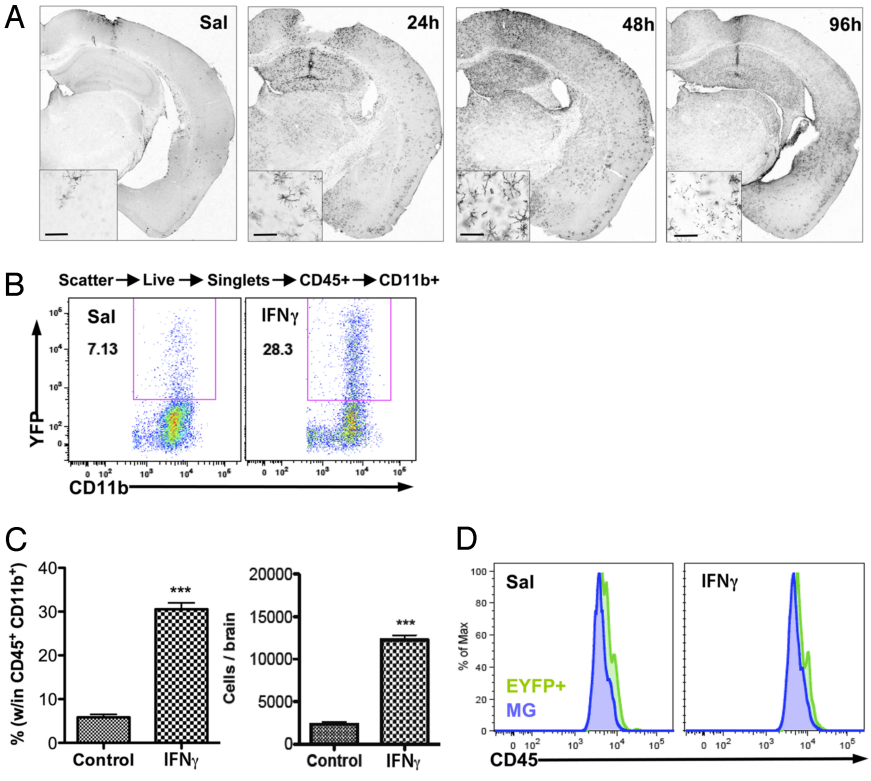

Fig. 1. IFNγ induces a large increase in resident bDC. CD11c/EYFP mice received i.c. injection of IFNγ (10 ng in 0.5 μl) in the CA1 region of hippocampus, and brains were processed for immunohistochemistry or FACS analysis. (*A*) Anti-GFP DAB immunohistochemistry brain sections of time course after IFNγ administration (Sal, 96 h). (Scale bars, 50 μm, *Insets*). (*B*) FACS analysis of EYFP$^+$ cells in saline (Sal) and IFNγ injected brains (2 days). (*C*) Graphed results showing percentage and total EYFP$^+$ cells per brain (n = 2–3 per group) (***, $P < 0.001$). (*D*) FACS analysis of CD45 levels in EYFP^{neg}MG and EYFP$^+$ cells.

ing the meninges and choroid plexus to reduce possible contamination by peripheral DC, showed that IFNγ induced a 5-fold increase (5.8% ± 0.7% vs. 30.5% ± 1.4%) in the number of EYFP$^+$bDC (3,368 ± 394 cells vs. 17,630 ± 836 cells) (Fig. 1 *B* and *C*). All EYFP$^+$bDC were CD45$^+$CD11b$^+$ (Fig. S1*A*), indicating their myeloid origin. Total numbers of CD45$^+$ cells in the brain were unchanged (Fig. S1*B*). Nonmyeloid leukocytes (CD45$^+$CD11b^{neg}EYFP^{neg} cells) increased slightly, in part because of a small increase in CD8$^+$ and CD4$^+$ T cells, but not to GR1$^+$ granulocytes or B19$^+$ B-cells (Fig. S1*C*), whereas total myeloid cells (CD45$^+$CD11b$^+$) did not change significantly. However, MG (CD45$^+$CD11b$^+$EYFP^{neg}) numbers declined after IFNγ (Fig. S1*B*). Notably, levels of CD45 were almost indistinguishable in MG and EYFP$^+$bDC (Fig. 1*D*). These results indicate that the high numbers of EYFP$^+$bDC induced by IFNγ were likely derived from a resident brain cell population rather than from infiltrating DC. To test this hypothesis, irradiated bone marrow chimeric animals were generated and analyzed.

EYFP$^+$bDC Are Radioresistant Cells. MG, which are radioresistant, populate the brain early in development and remain in the CNS with little replacement from bone marrow (BM)–derived cells in the adult (26). Using WT and CD11c/EYFP mouse BM chimeras (see *SI Materials*), we determined that, like the MG, bDC are radioresistant (Fig. S2). After irradiation and reconstitution with WT BM, EYFP$^+$bDC remained visible in regions where bDC are normally observed (Fig. S2*A* and *B* arrows), co-labeled with the MG marker Iba1, and displayed a ramified morphology similar to nonirradiated bDC (Fig. S2*A* and *B Lower*). These results suggest that bDC, like MG, do not require bone marrow replenishment. In contrast, brains from irradiated WT mice reconstituted with CD11c/EYFP$^+$ BM contained EYFP$^+$ cells, the dendritic morphology of which was similar, but not identical, to the finer dendritic and smaller cell-body morphology of bDC in nonirradiated mice (Fig. S2*C*).

IFNγ Drives Resident MG to Differentiate into EYFP$^+$bDC. Having established that bDC are radioresistant brain-resident cells, we used chimeric mice to determine whether the IFNγ-induced increase in EYFP$^+$bDC is mediated by an influx of BM-derived peripheral monocytes/DC or is derived from brain-resident cells. The results of this study showed that IFNγ induced a large increase of EYFP$^+$bDC in irradiated EYFP$^+$ (host) mice restored with WT BM (Fig. 2*A*), but not in the irradiated WT (host) mice restored with EYFP$^+$BM (Fig. 2*B*). Furthermore, flow-cytometric analysis of brains from irradiated WT (host) mice restored with EYFP$^+$BM confirmed the anatomic observations that although peripheral EYFP$^+$cells enter the brain after irradiation/reconstitution, this population is not increased after IC IFNγ injection (Fig. 2*C*). Furthermore, all BM-derived EYFP$^+$ donor cells had higher levels of CD45 compared with MG (Fig. 2*D*).

These results indicate that EYFP$^+$cells arising from IFNγ challenge come from a resident brain myeloid population. To address whether EYFP$^+$cell increase was caused by proliferation of EYFP$^+$bDC progenitor cells or by differentiation/activation of existing EYFP^{neg} cells, nonirradiated mice were injected intraperitoneally (i.p.) with the cell proliferation marker EdU during the IFNγ response and assayed 72 h later. Immunohistochemistry revealed rare co-labeling of EdU with EYFP$^+$cells (Fig. S3), indicating that the increase in EYFP$^+$cells could be attributed to the activation of a subset among the existing microglia.

bDC Demonstrate Migratory Capacity. Trafficking DC and other leukocytes rely on the expression of the chemokine receptor CCR7 (27). IFNγ-activated bDC upregulated CCR7 (Fig. 3*A*). This compelled us to examine whether activated bDC have migratory capabilities. Cultured bDC, primed with IFNγ for 2 h, were stereotaxically injected into the corpus callosum or the lateral ventricle (LV) of WT mice. Seven days later, EYFP$^+$ cell location was assessed in the brain. The bDC injected into the corpus callosum showed little migratory capacity (Fig. 3*B*) with no detectable EYFP$^+$ cells in other brain areas. However, bDC in the lateral

NEUROSCIENCE

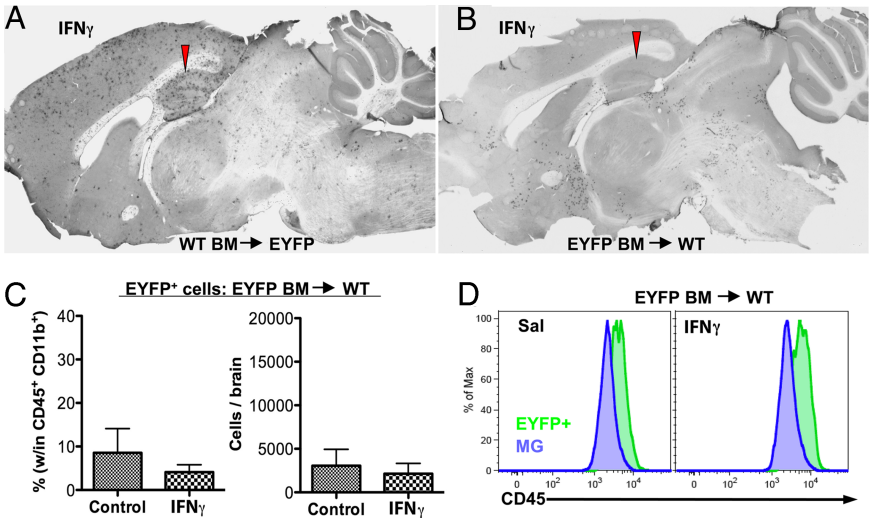

Fig. 2. CD11c/EYFP$^+$ cells induced by IFNγ are resident brain cells. WT or CD11c/EYFP recipient mice were lethally radiated, donor bone marrow (BM) from CD11c/EYFP or WT was administered i.v., and mice were allowed to recuperate for 7 weeks before they received i.c. injection of 10 ng IFNγ in the CA1. After 2 days, brains were processed for anti-GFP DAB immunohistochemistry or FACS analysis. (*A* and *B*) Photomicrographs of anti-GFP DAB IHC brain sections of sagittal ipsilateral hemispheres. (*C*) Quantification of the percentage (within CD45$^+$CD11b$^+$) and total number of EYFP$^+$ cells in WT recipient mice with EYFP$^+$ BM ($n = 2$ animals per group). (*D*) FACS analysis of CD45 levels in BM-derived EYFP$^+$cells and EYFP^{neg}MG.

ventricle were found caudal to the injection site, concentrated in the choroid plexus (Fig. 3*B*), a region recently shown to be a pivotal entry site of peripheral T cells into the noninflamed CNS (28).

IFNγ Induces MHC-II in bDC. MHC-II protein expression was studied after intracerebral (i.c.) IFNγ inoculation. Although there was no detectable expression of MHC-II in bDC in untreated brains (Fig. 4 *A* and *C*), IFNγ induced MHC-II protein expression in EYFP$^+$bDC and other cells (Fig. 4*B* and *D*). Further analysis of the CD45$^+$CD11b$^+$ brain population by flow cytometry revealed that IFNγ-induced MHC-II was predominant in EYFP$^+$bDC (Fig. 4*E*). Western blots of sorted MG and bDC from adult IFNγ-treated brains (Fig. 4*F*), or from primary brain cultures (Fig. 4*G*), demonstrated a positive correlation between the level of expression of EYFP and MHC-II induction ($r = 0.94$, $P = 0.0016$). Acute IFNγ challenge did not induce appreciable expression of co-stimulatory markers CD80, CD86, or CD40.

IL-4 Slightly Increases bDC but Does Not Induce MHC-II. IL-4 is reported to induce CD11c and MHC-II in cultured microglia (19).

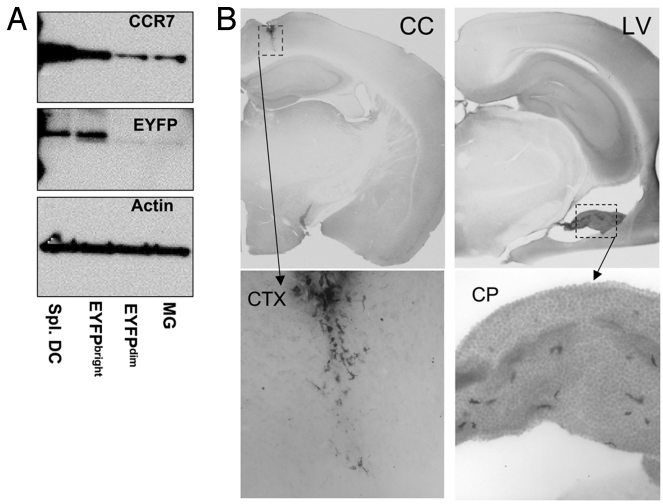

Fig. 3. IFNγ-activated bDC express CCR7 and migrate to choroid plexus. (*A*) CCR7/GFP/Actin Western blots of sorted EYFP$^+$spleen DC, EYFP$^+$bC, and EYFP^{neg}MG from IFNγ-treated brains. (*B*) Anti-GFP DAB IHC brain sections of WT brains injected in the corpus callosum (cc) or lateral ventricle (LV) with sorted and IFNγ-primed EYFP$^+$bDC from primary cultures ($n = 3$ mice per group). CP, choroid plexus; CTX, cortex. *Lower* are magnifications of boxed area above.

To test the effect of this cytokine in our system, CD11c/EYFP Tg mice were injected i.c. with IL-4 (10 ng in 0.5 μl). In contrast to IFNγ, induction of EYFP$^+$ cells by this dose of IL-4 was restricted only to the area near the injection site (Fig. 5*A*). Morphologically, IL-4–induced EYFP$^+$cells resembled activated MG (Fig. 5*A*); however, in sharp contrast to IFNγ, i.c. IL-4 did not induce MHC-II expression in bDC or in MG (Fig. 5*B Right*). Of note, IL-4 did induce MHC-II expression in meningeal Iba1$^+$EYFP^{neg} macrophages (MΦ) at the injection site/tract, as well as in choroid plexus DC and Iba$^+$MΦ (Fig. 5*B Right*). Also, IL-4 failed to induce MHC-II in cultured MG (Fig. 5*C*).

IFNγ-Activated bDC Are Functional Antigen Presenting Cells. Activated bDC and MG were sorted 2 days after i.c. IFNγ injection and co-cultured with SNARF-1–labeled naive CD4 OT-II T cells in the presence or absence of the model antigen OVA. Spleen DC derived from the same animals were used as positive controls. CD4 T-cell proliferation, assessed at 4 days by SNARF-1 dilution (Fig. 6*A*), showed that both IFNγ-activated bDC and MG caused antigen-specific proliferation of CD4 naive T cells at a APC:T-cell ratio of 1:3 (Fig. 6*A*); however, only the bDC induced elevated levels of Th1/Th17 cytokines (Fig. 6*B*). Moreover, when APC:T-cell ratios were decreased to 1:30 (Fig. 6*A*), bDC maintained their ability to induce proliferation of naive T cells, but not cytokine secretion, whereas MG showed a marked reduction in T-cell proliferation (Fig. 6*A*). Spleen DC induced greater T-cell proliferation under all conditions (Fig. 6*A*) but did not supersede T-cell cytokine production induced by activated bDC at the 1:3 ratio (Fig. 6*B*).

In addition to activating naive CD4 T cells, sorted bDC and MG were able to stimulate naive CD8 OT-I T cells in an OVA-antigen–dependent manner (Fig. S4). Both bDC and MG were similarly effective in stimulating CD8 T-cell proliferation (Fig. S4). This response was significantly reduced when either brain cell type was diluted to a 1:30 ratio (Fig. S4). As expected, spleen DC were more efficient at inducing CD8 T-cell proliferation than either bDC or MG at any dilution (Fig. S4).

Discussion

Antigen presenting cells (APC) in the CNS present an important topic for investigation, given their ability to direct immune responses. Infiltrating, bone marrow–derived DC contribute to various CNS chronic inflammatory conditions (8, 23, 24). However, distinguishing between infiltrating DC versus resident brain APC, and their respective contributions to disease, is essential for understanding brain-immune interactions, particularly as bone marrow–derived DC have a rapid turnover whereas brain

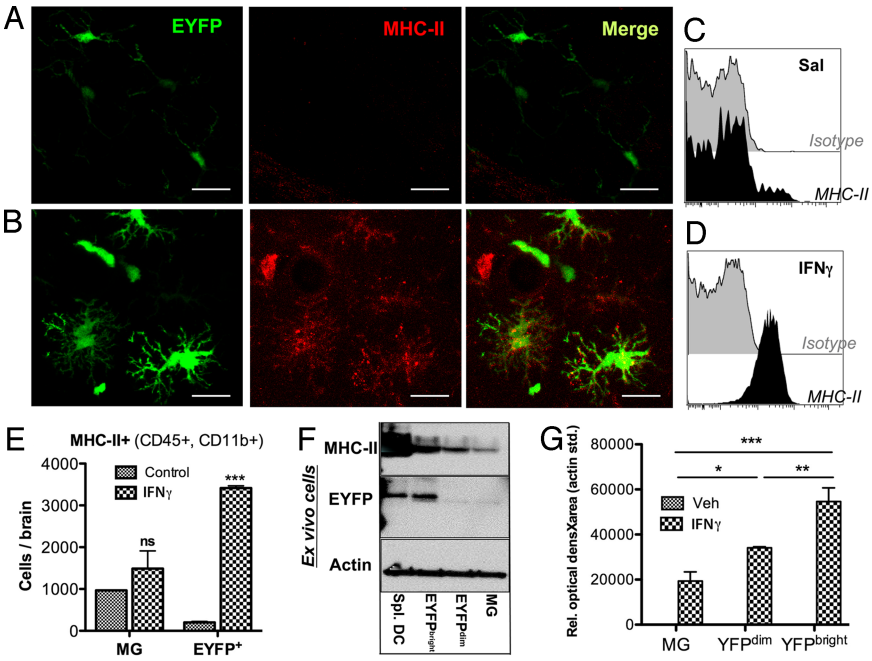

Fig. 4. IFNγ induces MHC-II preferentially in activated bDC. CD11c/EYFP mice received i.c. injection of 10 ng IFNγ in the CA1, and 2 days later brains were processed for IHC or FACS analysis. MHC-II immunofluorescence in the hippocampus of (*A*) saline (Sal) and (*B*) IFNγ-treated brains. (*C* and *D*) FACS analysis of MHC-II$^+$ cells within the EYFP$^+$ population. (*E*) Total number of MHC-II$^+$ cells in EYFP^{neg}MG and EYFP$^+$bDC. (*F*) MHC-II/GFP/Actin Western blots of sorted EYFP$^+$splenic DC, EYFP$^+$bDC, and EYFP^{neg}MG from IFNγ-treated brains. (*G*) Densitometry of MHC-II Western blot of sorted EYFP$^+$bDC and EYFP^{neg}MG from primary cultures stimulated for 3 days ± 10 ng/ml IFNγ. Graphs represent the means ± SEM ($n = 3$ mice or wells per group) (***, $P < 0.001$, **, $P < 0.01$, *, $P < 0.05$).

resident cells can be long lived. Supporting the existence of a brain-resident professional APC, we recently identified a population of CD11c/EYFP$^+$, CD11b$^+$ brain cells that we termed brain dendritic cells (bDC) (5). However, in the resting state, bDC may not be functional APC, as they do not express MHC-II. Aloisi et al. showed that APC properties can be induced in resting microglia via signals from preactivated T cells (29). Our current study shows that the Th1 cytokine IFNγ induced EYFP$^+$bDC from a subpopulation of MG. Defining specific markers for IFNγ-stimulated bDC, such as CCR7 and MHC-II, will facilitate their study in murine models that do not depend on CD11c/EYFP reporters.

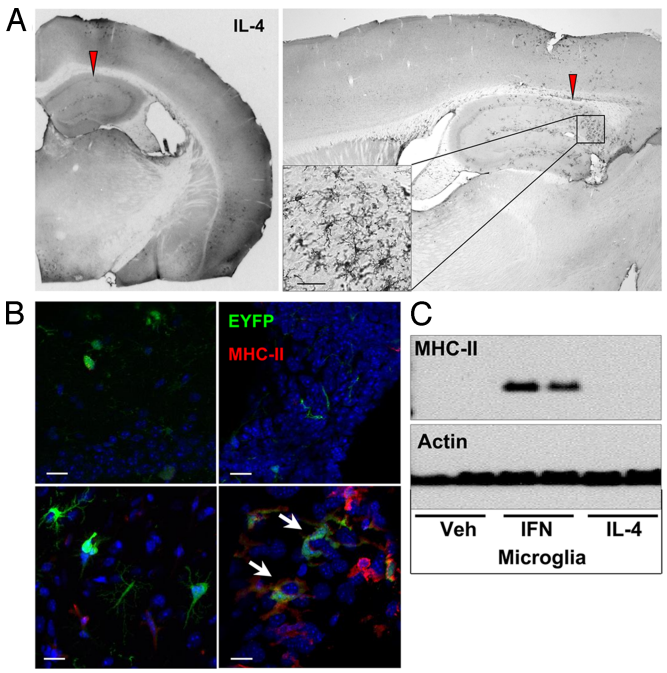

Fig. 5. IL-4 induces a small increase of bDC. CD11c/EYFP mice received i.c. injection of 10 ng IL-4 in the CA1 region of hippocampus, and brains were processed for immunohistochemistry. (*A*) Photomicrographs (×4–20) of anti-GFP DAB IHC coronal and sagittal section showing extent of EYFP$^+$ cell distribution and morphology from injection site 2 days after IL-4 challenge. (*B*) MHC-II immunofluorescence brain sections (*Upper*, saline; *Lower*, IL-4) showing parenchymal bDC (*Left*) vs. choroid plexus DC (*Right*). (Scale bar, 50 μm.) (*C*) MHC-II/Actin Western blot of primary MG stimulated for 3 days with 10 ng/ml IFNγ or IL-4.

Using mouse chimeras, we showed that IFNγ-activated bDC were of brain origin and not recruited from the bone marrow. Our results are supported by the findings that a 6-day brain infusion with IFNγ does not recruit peripheral DC, whereas GM-CSF causes a large infiltration of peripheral leukocytes and DC (24). Also consistent with our findings, Mausberg et al. report that IFNγ has its major impact on CD45^{int} MG, and has minor effects on other CD45^{high} leukocytes (24). In migration experiments, bDC were nonmotile in the corpus callosum but showed motility in the lateral ventricle. This could be caused by the large difference in space/fluidity between the two sites. It was unexpected, however, that EYFP$^+$bDC injected into ventricular cerebrospinal fluid (CSF) accumulated in the choroid plexus, given that CSF produced at this site flows away from this tissue. It can be speculated that bDC moved along the ventricle lining, possibly following a chemotactic gradient as recently demonstrated for T cells (28). Most striking is that bDC accumulated in this tissue, where encephalitogenic T cells enter the brain (28).

In addition to inducing EYFP$^+$bDC, IFNγ drove these cells into a competent, MHC-II$^+$, antigen-presenting state capable of activating naive CD4 T cells. IFNγ-mediated upregulation of CCR7 and MHC-II was restricted primarily to EYFP$^+$bDC, suggesting that these cells may represent the subpopulation of MG that express MHC-II in response to IFNγ in vivo described by Phillips et al. (18). Although previous studies show that IFNγ-treated MG do not induce naive T-cell proliferation and do not efficiently stimulate memory T cells (11, 12), by selecting the IFNγ-activated bDC population, we showed that this subpopulation was capable of stimulating naive CD4 T cells in an antigen-dependent fashion. It will be important in future studies to address whether bDC are effective APC in vivo and in the setting of nontransgenic T cells.

It was striking that bDC were the only APC capable of inducing IL-17 secretion in T-cell co-cultures. Th17 T cells are implicated in neuroinflammation, particularly in multiple sclerosis and experimental autoimmune encephalitis (EAE). In fact during EAE, T-cell

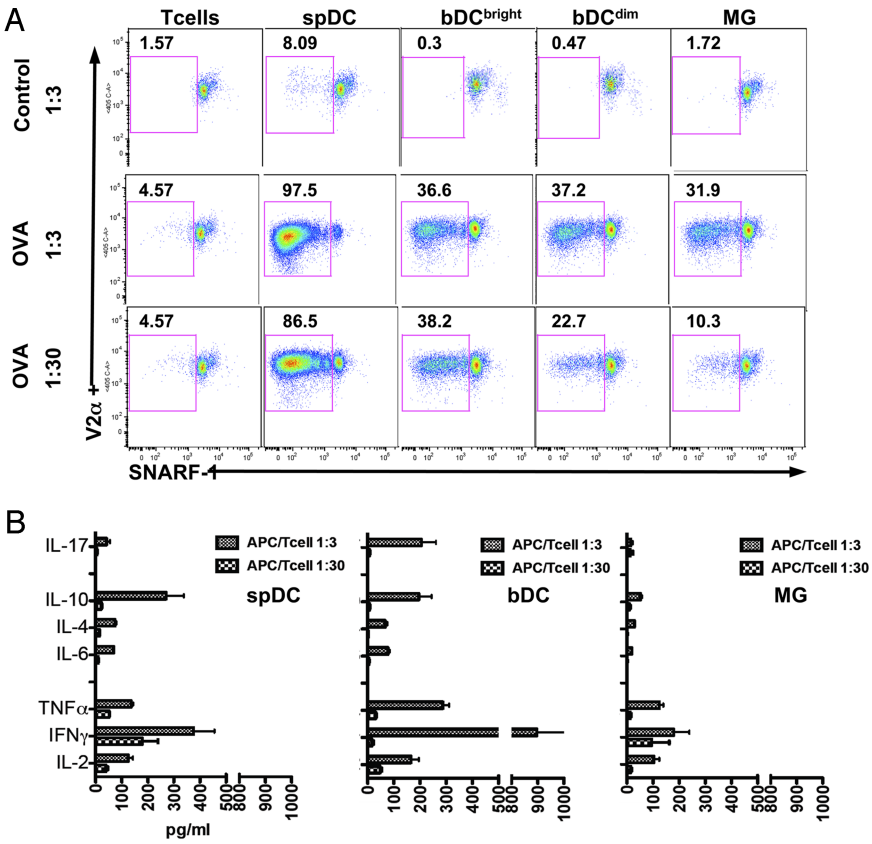

Fig. 6. IFNγ-activated bDC are capable of antigen-specific CD4 T-cell activation. CD11c/EYFP mice received i.c. injection of IFNγ. Two days later, EYFP^{+}bDC and EYFP^{neg}MG were sorted and co-cultured for 4 days with naive OT-II T cells at a ratio of 1:3 and 1:30. (*A*) Dot plots gated on Singlets/Live/CD3^{+}CD4^{+}V2α^{+} T cells showing SNARF-1 dilution (one representative experiment of four). (*B*) Cytokine expression profiles of OT-II T-cell cultures. (Graphs are from one representative experiment of two in triplicate).

infiltration and inflammation in the brain parenchyma only occurs when Th17 cells outnumber Th1 cells (30), and IFNγ signaling in the CNS is required for parenchymal inflammation (31). These findings are consistent with our results, and suggest that bDC are potential therapeutic targets for inflammation. EYFP^{neg}MG expressed significantly less MHC class II and were not as efficient APC as bDC. Interestingly, both IFNγ-activated bDC and MG stimulated naive CD8 T cells, although only at a high APC:T-cell ratio, as previously reported for MG (32).

Our choice of using IFNγ and IL-4 was based on literature showing that invading leukocytes are the main source of these important immune cytokines in the brain (33, 34). IFNγ has been shown by others to exert functional effects on resident MG and to alter the course of immune responses. In fact, leukocyte-derived IFNγ can regulate MG chemokine release patterns in the course of bacterial meningitis or EAE (35, 36). However, it is still unclear whether IFNγ initiates a detrimental or neuroprotective effect on the brain. For example, during the induction phase of EAE, T-cell–derived IFNγ interacts with CNS cells to suppress inflammation and pathogenesis (31). Likewise, IFNγ prevents neuronal death after CD8 T-cell responses in the brain (37). Specifically, small amounts IFNγ induce MG to preserve neural tissue, whereas high doses render them neurotoxic (38). Here we show that a single exposure to low-dose IFNγ had a profound effect on brain MG by inducing a subpopulation to become bDC and functional APC. On the other hand, the Th2 cytokine, IL-4 had a very limited effect on inducing CD11c/EYFP expression and did not stimulate detectable levels of MHC-II in either bDC or MG.

One significant question raised by EAE research is the identity of the brain APC that re-stimulates the first/early encephalitogenic T cells that lead to disease pathology (28, 39). Our data strongly suggest that activated bDC may be a candidate for the resident, parenchymal APC required for encephalitogenic T-cell reactivation, as IFNγ-activated bDC were capable of inducing antigen-specific CD4 T cells and producing Th1/Th17 cytokines. Future studies will address the potential role of antigen presentation in the normal and pathological brain and will help to guide the development of therapies to enhance desirable responses to tumors or infections (40) or to suppress unwanted autoimmunity.

Methods

Animals. The transgenic mouse line CD11c/EYFP (C57BL6/J background) was used, in which EYFP expression is driven by the CD11c gene (4). T cells were obtained from young OT-I and OT-II (C57BL6/J background) mice purchased from Jackson Laboratories (for TCR description of these mice, see *SI Materials*). Animals were bred in Rockefeller University facilities under 12:12 light:dark cycle with free access to chow and water. All experimental procedures were approved by the Rockefeller University Animal Care and Use Committee.

Chimeras. See *SI Materials*.

Unilateral Stereotaxic Intracerebral Injections. Anesthetized mice were placed in a stereotaxic frame and, using a 10-μl microsyringe (WPI 500819), cytokines (see *SI Materials*) were infused in the CA1 area (Bregma coordinates: rostro-caudal −2.3; medial-lateral −2.7; dorso-ventral −2.2) over a 2-min period. The needle was left in place for another 5 min before slow withdrawal (45 s). Inoculated mice were singly housed with water and food ad libitum.

Immunofluorescence and Immunohistochemistry. Free-floating sections were rinsed in TBS, blocked in 0.5% bovine serum albumin (BSA) in tris-buffered saline (TBS) and incubated overnight at 4 °C with primary antibodies (see table *SI Materials*) in 0.1% BSA, 0.1% Triton TBS. After washing, sections were incubated for 1 h at room temperature with secondary fluorescent antibodies (for immunofluorescence) or biotin-labeled antibody (for immunohistochemistry). Biotin-immune complexes were detected using the ABC and diaminobenzidine (DAB) peroxidase substrate kit (Vector, Burlingame, CA). A Nikon Optiphot Microscope or light box with a Coolpix Digital camera was used for light microscopy image acquisition. Fluorescent images were acquired using an LSM510 confocal Zeiss Axioplan microscope (Rockefeller University Bioimaging Facility).

EdU Proliferation. See *SI Materials*.

Cell Isolation by Fluorescence-Activated Cell Sorting. Slight variations on reported methods (41) were used to obtain enriched brain mononuclear cells by fluorescence-activated cell sorting (FACS). In brief, adult mice 2–3 months old were rapidly decapitated, their brains were extracted, and meninges, blood vessels and choroid plexus were carefully removed under a dissecting scope on ice-cold Hank's balanced salt solution HBSS buffer. Brain cell suspensions, obtained by gentle triturating with frosted-glass slides, were incubated with type II-S collagenase (600U; Roche), Dispase II (0.5%; Roche), and DNase (450U; Invitrogen) for 30 min at 37 °C in 15 ml HBSS with $CaMg^{2+}$. After digestion, cell suspensions were gently pipetted with fire-polished Pasteur pipettes, washed, and subjected to a 70–37% Percoll gradient centrifugation at 1,600 *g* for 30 min at 25 °C. Cells were collected from the 37/70 interphase; in addition, many $EYFP^{+}$ cells were found in the myelin-rich phosphate-buffered saline (PBS)/37 interphase. Enriched cells were washed in 5% FBS-PBS, stained for CD45, CD11b and DAPI, and sorted in a FACS Aria Flow Cytometer (BD).

FACS Analysis. Percoll gradient enriched cells were rinsed in 5% FCS PBS (FACS buffer), blocked with anti-FC block for 15min at 4 °C, and then stained with fluorophore-conjugated primary antibodies (see Table S1) for 15 min at 4 °C. After washing, cells were acquired using a BD LSR-II FACS analyzer using FACS Diva software. Gates and compensations were set using isotype controls and FMO antibody combinations. Postacquisition data analysis was carried out using FlowJo software (TreeStar, Ashland, OR).

T-Cell Proliferation Assay. SNARF-1 (42) labeled OT-I or OT-II T cells, obtained by negative selection using DYNA beads (see *SI Materials*), were seeded at 10^5 cells/well in a 96-well, round-bottom plate in R5 media (5% FCS+Penn/Strep RPMI) supplemented with 0.5 μM β-mercaptoethanol. Sorted $EYFP^{+}$bDC, $EYFP^{neg}$MG, or $EYFP^{+}$splenic DC (from the same animals) were co-cultured with the T cells at various ratios and incubated at 37 °C in 5% CO_2 for 4 days with or without 100 μg/ml OVA, or 40 μg/ml TCR peptide as positive control. Cells were then stained with Live/Dead Fixable Aqua (Molecular Probes, L34957) and T-cell antibody markers, and proliferation was assessed by SNARF-1 dilution (42) using an LSR-II FACS analyzer gating on live (Aqua negative), $EYFP^{neg}$, $CD3^{+}$, $CD4^{+}$ (for OT-II), $CD8^{+}$ (for OT-I) and V2α-TCR^{+} cells. Cytokines were measured in the supernatants from the T-cell cultures using the BD Th1/Th2/Th17 CBA cytokine kit following the manufacturer's instructions (BD 560485).

Primary Microglia/bDC Cultures. See *SI Materials*.

Western Blotting. See *SI Materials*.

Statistical Analysis. Statistical analysis was performed using Prism (GraphPad, La Jolla, CA). Experiments involving two groups were compared using a Student *t* test. Experiments involving more than two groups were compared by ANOVA, followed by Tukey post hoc analysis. Graphs show the mean ± standard error of the mean (SEM). A value of $P < 0.05$ was considered statistically significant. *, $P < 0.05$, **, $P < 0.01$,***, $P < 0.0001$.

ACKNOWLEDGMENTS. Support for this research was provided by Woodin Dendritics, LLC and a gift from the Peter Deane Trust. FACS support was provided by the Empire State Stem Cell fund through New York State Department of Health Contract #C023046. The authors extend special thanks to Judit Gal-Toth for animal colony maintenance and excellent technical assistance; to the RU Comparative Bioscience Center (CBC), Flow Cytometry Resource Center, and the Bioimaging Resource Center for expert technical assistance; to Kate Moffit, David Einheber and Haley Vecchiarelli for help with tissue processing; and to members of the McEwen laboratory, and Drs. Ralph Steinman and Melvin Cohn for valuable discussions and support.

1. Steinman RM, Banchereau J (2007) Taking dendritic cells into medicine. *Nature* 449:419–426.
2. Shortman K, Liu YJ (2002) Mouse and human dendritic cell subtypes. *Nat Rev Immunol* 2:151–161.
3. McMenamin PG (1999) Distribution and phenotype of dendritic cells and resident tissue macrophages in the dura mater, leptomeninges, and choroid plexus of the rat brain as demonstrated in wholemount preparations. *J Comp Neurol* 405:553–562.
4. Lindquist RL, Shakhar G, Dudziak D, Wardemann H, Eisenreich T, et al. (2004) Visualizing dendritic cell networks in vivo. *Nat Immunol* 5:1243–1250.
5. Bulloch K, Miller MM, Gal-Toth J, Milner TA, Gottfried-Blackmore A, et al. (2008) CD11c/EYFP transgene illuminates a discrete network of dendritic cells within the embryonic, neonatal, adult, and injured mouse brain. *J Comp Neurol* 508:687–710.
6. Schwartz M, Butovsky O, Bruck W, Hanisch UK (2006) Microglial phenotype: Is the commitment reversible? *Trends Neurosci* 29:68–74.
7. Ford AL, Goodsall AL, Hickey WF, Sedgwick JD (1995) Normal adult ramified microglia separated from other central nervous system macrophages by flow cytometric sorting. Phenotypic differences defined and direct ex vivo antigen presentation to myelin basic protein-reactive CD4+ T cells compared. *J Immunol* 154:4309–4321.
8. Fischer HG, Reichmann G (2001) Brain dendritic cells and macrophages/microglia in central nervous system inflammation. *J Immunol* 166:2717–2726.
9. Santambrogio L, Belyanskaya SL, Fischer FR, Cipriani B, Brosnan CF, et al. (2001) Developmental plasticity of CNS microglia. *Proc Natl Acad Sci USA* 98:6295–6300.
10. Aloisi F, De Simone R, Columba-Cabezas S, Penna G, Adorini L (2000) Functional maturation of adult mouse resting microglia into an APC is promoted by granulocyte-macrophage colony-stimulating factor and interaction with Th1 cells. *J Immunol* 164:1705–1712.
11. Aloisi F, Ria F, Columba-Cabezas S, Hess H, Penna G, Adorini L (1999) Relative efficiency of microglia, astrocytes, dendritic cells and B cells in naive CD4+ T-cell priming and Th1/Th2 cell restimulation. *Eur J Immunol* 29:2705–2714.
12. Aloisi F, Ria F, Penna G, Adorini L (1998) Microglia are more efficient than astrocytes in antigen processing and in Th1 but not Th2 cell activation. *J Immunol* 160:4671–4680.
13. Suzuki S, Honma K, Matsuyama T, Suzuki K, Toriyama K, et al. (2004) Critical roles of interferon regulatory factor 4 in CD11bhighCD8alpha-dendritic cell development. *Proc Natl Acad Sci USA* 101:8981–8986.
14. Hayes GM, Woodroofe MN, Cuzner ML (1987) Microglia are the major cell type expressing MHC class II in human white matter. *J Neurol Sci* 80:25–37.
15. Merrill JE, Benveniste EN (1996) Cytokines in inflammatory brain lesions: Helpful and harmful. *Trends Neurosci* 19:331–338.
16. Neumann H, Cavalie A, Jenne DE, Wekerle H (1995) Induction of MHC class I genes in neurons. *Science* 269:549–552.
17. Sethna MP, Lampson LA (1991) Immune modulation within the brain: Recruitment of inflammatory cells and increased major histocompatibility antigen expression following intracerebral injection of interferon-gamma. *J Neuroimmunol* 34:121–132.
18. Phillips LM, Simon PJ, Lampson LA (1999) Site-specific immune regulation in the brain: Differential modulation of major histocompatibility complex (MHC) proteins in brainstem vs. hippocampus. *J Comp Neurol* 405:322–333.
19. Butovsky O, Talpalar AE, Ben-Yaakov K, Schwartz M (2005) Activation of microglia by aggregated beta-amyloid or lipopolysaccharide impairs MHC-II expression and renders them cytotoxic whereas IFN-gamma and IL-4 render them protective. *Mol Cell Neurosci* 29:381–393.
20. Lampson LA (1995) Interpreting MHC class I expression and class I/class II reciprocity in the CNS: Reconciling divergent findings. *Microsc Res Tech* 32:267–285.
21. Butovsky O, Koronyo-Hamaoui M, Kunis G, Ophir E, Landa G, et al. (2006) Glatiramer acetate fights against Alzheimer's disease by inducing dendritic-like microglia expressing insulin-like growth factor 1. *Proc Natl Acad Sci USA* 103:11784–11789.
22. Greter M, Heppner FL, Lemos MP, Odermatt BM, Goebels N, et al. (2005) Dendritic cells permit immune invasion of the CNS in an animal model of multiple sclerosis. *Nat Med* 11:328–334.
23. Bailey SL, Schreiner B, McMahon EJ, Miller SD (2007) CNS myeloid DCs presenting endogenous myelin peptides 'preferentially' polarize CD4+ T(H)-17 cells in relapsing EAE. *Nat Immunol* 8:172–180.
24. Mausberg AK, Jander S, Reichmann G (2009) Intracerebral granulocyte-macrophage colony-stimulating factor induces functionally competent dendritic cells in the mouse brain. *Glia* 57:1341–1350.
25. Raivich G, Bohatschek M, Kloss CU, Werner A, Jones LL, Kreutzberg GW (1999) Neuroglial activation repertoire in the injured brain: Graded response, molecular mechanisms and cues to physiological function. *Brain Res Brain Res Rev* 30:77–105.
26. Davoust N, Vuaillat C, Androdias G, Nataf S (2008) From bone marrow to microglia: Barriers and avenues. *Trends Immunol* 29:227–234.
27. Forster R, Davalos-Misslitz AC, Rot A (2008) CCR7 and its ligands: Balancing immunity and tolerance. *Nat Rev Immunol* 8:362–371.
28. Reboldi A, Coisne C, Baumjohann D, Benvenuto F, Bottinelli D, et al. (2009) C-C chemokine receptor 6-regulated entry of TH-17 cells into the CNS through the choroid plexus is required for the initiation of EAE. *Nat Immunol* 10:514–523.
29. Aloisi F, Serafini B, Adorini L (2000) Glia-T cell dialogue. *J Neuroimmunol* 107:111–117.
30. Stromnes IM, Cerretti LM, Liggitt D, Harris RA, Goverman JM (2008) Differential regulation of central nervous system autoimmunity by T(H)1 and T(H)17 cells. *Nat Med* 14:337–342.
31. Lees JR, Golumbek PT, Sim J, Dorsey D, Russell JH (2008) Regional CNS responses to IFN-gamma determine lesion localization patterns during EAE pathogenesis. *J Exp Med* 205:2633–2642.
32. Beauvillain C, Donnou S, Jarry U, Scotet M, Gascan H, et al. (2008) Neonatal and adult microglia cross-present exogenous antigens. *Glia* 56:69–77.
33. Merrill JE, Kono DH, Clayton J, Ando DG, Hinton DR, Hofman FM (1992) Inflammatory leukocytes and cytokines in the peptide-induced disease of experimental allergic encephalomyelitis in SJL and B10.PL mice. *Proc Natl Acad Sci USA* 89:574–578.
34. Renno T, Krakowski M, Piccirillo C, Lin JY, Owens T (1995) TNF-alpha expression by resident microglia and infiltrating leukocytes in the central nervous system of mice with experimental allergic encephalomyelitis. Regulation by Th1 cytokines. *J Immunol* 154:944–953.
35. Hausler KG, Prinz M, Nolte C, Weber JR, Schumann RR, et al. (2002) Interferon-gamma differentially modulates the release of cytokines and chemokines in lipopolysaccharide- and pneumococcal cell wall-stimulated mouse microglia and macrophages. *Eur J Neurosci* 16:2113–2122.
36. Tran EH, Prince EN, Owens T (2000) IFN-gamma shapes immune invasion of the central nervous system via regulation of chemokines. *J Immunol* 164:2759–2768.
37. Richter K, Hausmann J, Staeheli P (2009) Interferon-gamma prevents death of bystander neurons during CD8 T-cell responses in the brain. *Am J Pathol* 174:1799–1807.
38. Schwartz M, Yoles E (2006) Immune-based therapy for spinal cord repair: Autologous macrophages and beyond. *J Neurotrauma* 23:360–370.
39. Goverman J (2009) Autoimmune T-cell responses in the central nervous system. *Nat Rev Immunol*, in press.
40. Dutta T, Spence A, Lampson LA (2003) Robust ability of IFN-gamma to upregulate class II MHC antigen expression in tumor bearing rat brains. *J Neurooncol* 64:31–44.
41. Sierra A, Gottfried-Blackmore AC, McEwen BS, Bulloch K (2007) Microglia derived from aging mice exhibit an altered inflammatory profile. *Glia* 55:412–424.
42. Magg T, Albert MH (2007) Tracking cell proliferation using the far red fluorescent dye SNARF-1. *Cytometry B Clin Cytom* 72:458–464.